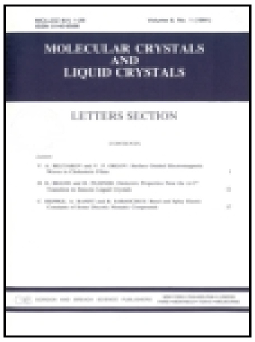

Molecular Crystals and Liquid Crystals

ISSN: 1542-1406 (Print) 1563-5287 (Online) Journal homepage: http://www.tandfonline.com/loi/gmcl20

Characteristics of Dye-Sensitized Solar Cells Using TiO_2 Nanotube Arrays with Large Surface Area by Spin-Coating Nanoparticle

Jun Hyuk Yang, Kyung Hwan Kim, Chang Seob Kim & Hyung Wook Choi

To cite this article: Jun Hyuk Yang, Kyung Hwan Kim, Chang Seob Kim & Hyung Wook Choi (2015) Characteristics of Dye-Sensitized Solar Cells Using TiO_2 Nanotube Arrays with Large Surface Area by Spin-Coating Nanoparticle, Molecular Crystals and Liquid Crystals, 620:1, 91-99, DOI: 10.1080/15421406.2015.1094882

To link to this article: http://dx.doi.org/10.1080/15421406.2015.1094882

Mol. Cryst. Liq. Cryst., Vol. 620: pp. 91–99, 2015
Copyright © Taylor & Francis Group, LLC
ISSN: 1542-1406 print/1563-5287 online
DOI: 10.1080/15421406.2015.1094882

Characteristics of Dye-Sensitized Solar Cells Using TiO_2 Nanotube Arrays with Large Surface Area by Spin-Coating Nanoparticle

JUN HYUK YANG,[1] KYUNG HWAN KIM,[1]
CHANG SEOB KIM,[2] AND HYUNG WOOK CHOI[1,*]

[1]Department of Electrical Engineering, Gachon University, Sujeong-Gu, Seongnam-Si, Gyeonggi-Do, Korea
[2]Department of Energy IT, Gachon University, Sujeong-Gu, Seongnam-Si, Gyeonggi-Do, Korea

Highly ordered TiO_2 nanotube arrays (TNAs) fabricated by anodization are very attractive for use in dye-sensitized solar cells (DSSCs), because of their superior charge percolation and slow charge recombination. Highly ordered, vertically aligned TNAs have been prepared by three-step anodic oxidation. In this work, we investigated such strategies for improving the efficiency of DSSCs. Based on one of these approaches, oxide semiconductors in the form of a TNA were used as a novel method for improving electron transport through a film. A solution containing an appropriate amount of TiO_2 nanoparticles was prepared, and the mixed slurry was spin-coated on a TNA film. The coated film provided a large surface area for dye adsorption. The DSSCs achieved a light-to-electric energy conversion efficiency of 5.91% under simulated solar irradiation at 100 mW/cm^2 (AM 1.5).

Keywords DSSC; TiO_2; TiO_2 nanoparticle; TiO_2 nanotube; spin-coating; photoelectrode

Introduction

Since their discovery in 1991, dye-sensitized solar cells (DSSCs) have been extensively studied as alternatives to silicon-based solar cells because of their simple structure, transparency, flexibility, low production costs, and wide range of applications. Despite these advantages, the low efficiency of DSSCs compared with those of silicon-based solar cells limits their commercial implementation.[1–4] Consequently, there is a critical need to improve the efficiency of state-of-the-art DSSCs to enable the development of next-generation solar cells. DSSCs consist of four parts: (1) the TiO_2 electrode film layer, covered by a monolayer of dye molecules that absorb solar energy; (2) the transparent conductive oxide layer, which facilitates charge transfer from the electrode layer; (3) the counter electrode layer, made of Pt or C; and (4) the redox electrolyte layer for reducing the level of energy

---

[*] Address correspondence to Prof. HyungWook Choi, Department of Electrical Engineering, Gachon University, 1342 Seongnam Daero, Sujeong-Gu, SeongNam-Si, Gyeonggi-Do 461-701, Korea (ROK). E-mail: chw@gachon.ac.kr

Color versions of one or more of the figures in the article can be found online at www.tandfonline.com/gmcl.

supplied from the dye molecules.[5,6] Research efforts to improve the efficiency of DSSCs have therefore been primarily focused on improvements to the DSSC components.[7] Generally, DSSCs are fabricated using TiO_2 nanoparticles (TNPs).[8–11] Although one of the important features of DSSCs is the mesoporous film of interconnected TNPs, which can provide large surface areas for adsorption of a large amount of dye molecules, the performance of a DSSC is still limited by electron transport in the nanocrystal boundaries and electron recombination with the electrolyte during electron migration. Many researchers have reported that one-dimensional nanostructures can be used in DSSCs instead of nanoparticles, to facilitate electron transfer.[12–20] In addition to their unusual electronic properties, one-dimensional TiO_2 nanostructures function as light-scattering materials with minimum sacrifice of surface area. However, the fatal flaw of one-dimensional nanostructures is their insufficient dye adsorption, resulting from their small specific surface areas. The main challenge is to achieve a balance between a large specific surface area and low transmission.

In this work, we investigated the above strategies for improving the efficiency of DSSCs. Based on one of these approaches, oxide semiconductors in the form of TiO_2 nanotube arrays (TNAs) were used as a novel means of improving electron transport through a film. A one-dimensional conduction path was added through the three-dimensional conduction path, to increase the electron-transport speed and enhance the light-scattering ability. A solution containing an appropriate amount of TNPs was prepared, and the mixed slurry was spin-coated on a TNA film. The coated film provided a large surface area for dye adsorption.

Experimental

1. Preparation of TiO_2 Nanotube Array Layers

The TNAs were prepared using an optimized three-step anodization process.[21,22] Ti foil (0.25 mm thick, 99.7% purity, Aldrich) of area 2 cm × 3 cm was degreased by ultrasonic agitation in acetone, isopropanol, and deionized (DI) water, for 30 min each, and then dried with N_2 gas. The ethylene glycol electrolyte contained 0.25 wt% NH_4F (98%, Aldrich) and 2 vol% DI water. The anodization was performed in a two-electrode system in which the Ti foil served as the working electrode and a Pt plate (2 cm × 3 cm) served as the counter electrode. Anodization was conducted at 0–4°C at a constant voltage of 60 V for 1 h. The prepared TNAs were then removed by sonication for 5 min in DI water. The second step in the anodization was carried out under the same conditions. The mean thickness of the prepared TNAs was 13 μm and 22 μm, respectively. The TNA length was controlled by the input voltage time. The prepared amorphous TNAs were crystallized in the anatase phase at 450°C for 1 h in air at a heating rate of 1°C/min. After another anodization step under the same conditions for 10 min and then immersion in a H_2O_2 solution (33%) for 10 min, the anatase TNAs were detached from the Ti substrate. After rinsing and drying, the self-standing TNAs were cut into 5 mm × 5 mm squares for transfer.

2. Preparation of TiO_2 Layer and Slurry Spin-Coating

A TiO_2 paste was prepared as described in the literature.[23,24] The TiO_2 paste was coated on fluoride-doped tin oxide (FTO) glass using the doctor-blade method. The TNA film was then transferred onto the FTO glass. The prepared TiO_2 film was sintered at 450°C for 1 h in air. We also prepared a slurry consisting of TiO_2 particles (10 nm, 20 nm, 6 g;

anatase 99.99%, Aldrich) in a solution of ethanol (90 mL), acetic acid (1 mL), α-terpineol (20 mL), and DI water (10 mL). The mixture was stirred well at room temperature for 2 h, and then ultrasonicated for 2 h, to give a slurry. The slurry was spin-coated onto the prepared TiO_2 film. Heat treatment at 450°C produced a TiO_2 photoelectrode film. A Pt catalyst electrode was prepared by mixing H_2PtCl_6 (5 mM) with isopropanol, followed by ultrasonic treatment. A counter electrode, which facilitates the redox reaction of the electrolyte, was fabricated by spin-coating the prepared H_2PtCl_6 solution at 1000 rpm for 30 s, followed by heat treatment at 450°C for 30 min.

3. *Assembly of Dye-Sensitized Solar Cells*

The dye solution for adsorption on the electrode films was prepared by mixing 0.5 mM Ru dye (N719, Solaronix) with ethanol. To facilitate adsorption of the dye molecules, the prepared TiO_2 electrode films were soaked in the dye solution in darkness for 24 h. Finally, DSSCs were fabricated by sandwiching the prepared electrode films and counter electrodes at 120°C for 10 min, using a hot-melt sealant (60°C). The electrolyte (I^-/I_3^-) was injected between the two electrodes via an inlet and then sealed with a cover glass (figure 1).

4. *Characterization*

The phases of the TNPs and TNAs obtained by anodization were identified by X-ray diffraction (XRD), using a Rigaku D/MAX-2200 diffractometer with a Cu Kα radiation source. The morphologies of the prepared TiO_2 films were investigated using field-emission scanning electron microscopy (FE-SEM; Hitachi S-4700) and the absorbances of the prepared TiO_2 electrode films were measured using an ultraviolet-visible (UV-vis) spectrometer (UV-Vis 8453, Agilent). The conversion efficiencies of the fabricated DSSCs were determined using a current–voltage (*I–V*) solar simulator (McScience K3400), and electrochemical impedance spectroscopy (EIS; McScience K3000). The active area of the resulting cell exposed to light was approximately 0.25 cm^2 (0.5 cm × 0.5 cm).

Results and Discussion

Figure 2(a) shows the XRD pattern of the Ti foil (JCPDS No. 44-1294). After anodization, the TNAs that were peeled off from the Ti substrate were examined using XRD. Figure 2(b) shows the XRD pattern of the TNAs fabricated by calcination at 450°C.

The diffraction peaks are in good agreement with those in the standard JCPDS cards of anatase TiO_2 (No. 21-1272). The XRD pattern of the TNAs shows prominent (101), (004), and (200) anatase peaks. To improve the DSSC efficiency, it is preferable to produce TiO_2 phase containing anatase only.[25,26]

Figure 3(a) shows the SEM images of cross-sectional views of the TNAs. The TNA length was about 13 μm. Few cracks, a uniform tubular structure, and vertical orientation to the film surface are observed. Anodic oxidation under the present conditions gave TNAs of length about 22 μm, as shown in Figure 3(b). Figure 3(c) shows that the TNA diameter is about 100 nm, and the TNA surface is uniform. Figure 3(d) shows the SEM images of TNPs deposited on the TNA surface by spin-coating. The inset in Figure 3(d) shows that the TNAs are filled with TNPs.

Figure 4 shows the absorption spectra of the N-719 dye in the 400–800 nm wavelength range for various TiO_2 film samples. At 400–500 nm, the photoelectrode with 10 nm TNPs spin-coated on 22 μm TNAs showed the highest absorbance. According to

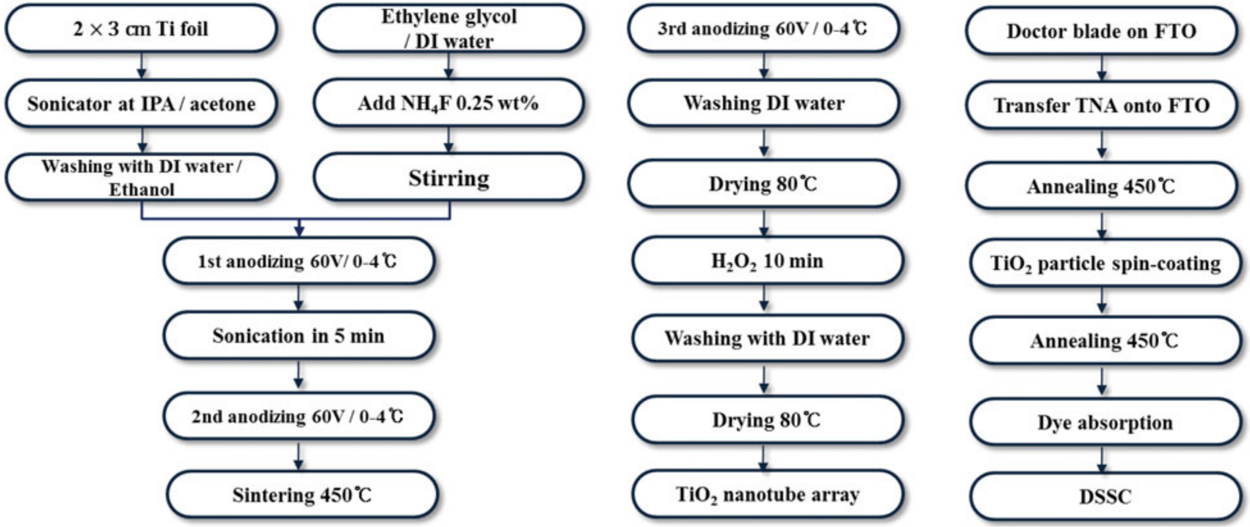

Figure 1. Flow chart of DSSC manufacture.

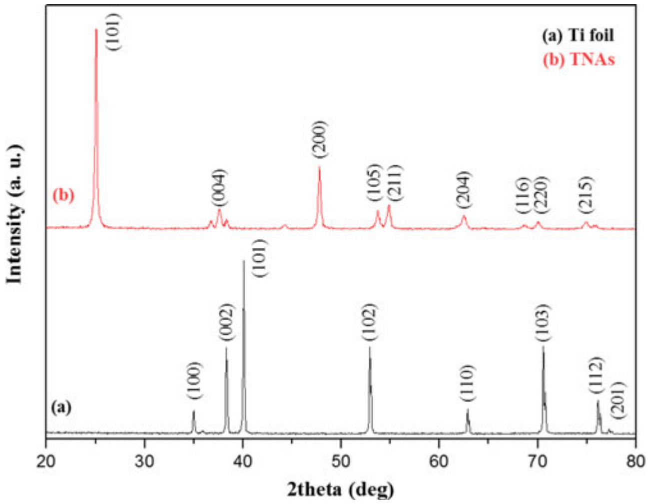

Figure 2. XRD patterns of (a) Ti foil and (b) TNAs.

the Lambert–Beer law, a higher absorbance means a higher dye concentration. The photoelectrode prepared by spin-coating 10 nm TNPs on 22 μm TNAs provides a large surface area for dye adsorption. The TiO_2 layer with the dye serves as a photoactive layer. The

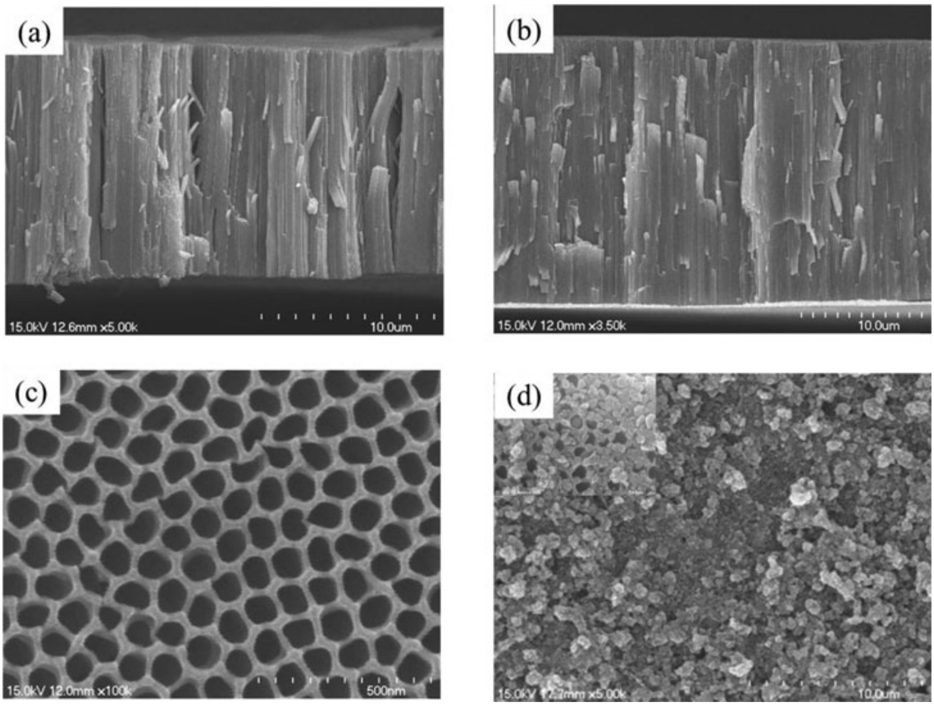

Figure 3. FE-SEM images of (a, b) cross-sections of TNAs, (c) surface of TNAs, (c) surface of second-anodization-step TNAs, and (d) TNP-coated TiO_2 film; inset in (d) shows TNA surface.

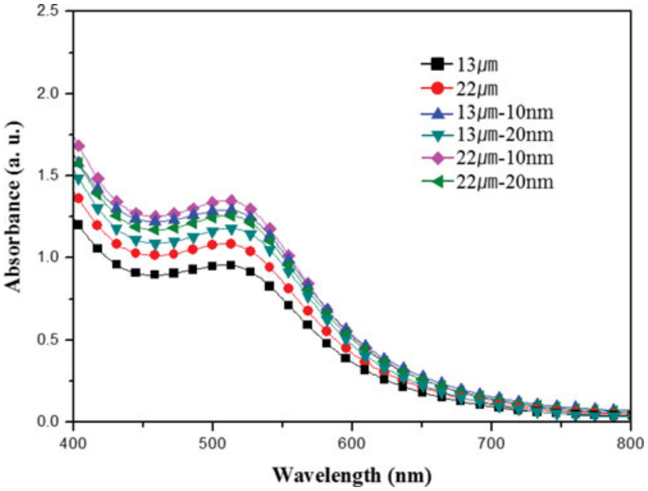

Figure 4. UV-vis absorbances of various TiO_2 films.

photocurrent of a DSSC correlates directly with the number of dye molecules: a larger number of adsorbed dye molecules results in more incident light being harvested, and, consequently, a larger photocurrent.

Figure 5 shows the EIS analysis of DSSCs fabricated using various photoelectrodes. The spectra provide information on electron transport and recombination in the DSSCs. EIS is a useful method for the analysis of charge-transport processes and internal resistances.[27] The observed decrease in the charge-transfer resistance (R_{CT}) of the photoelectrode consisting of 10 nm TNPs spin-coated on 22 μm TNAs indicates a reduction in the electron recombination rate and an increase in the electron-transport efficiency. As shown in Figure 5, R_{CT} decreases with increasing absorbance of the sample. This increases the number of electrons injected into the TiO_2 film, improves the electrical conductivity, and reduces

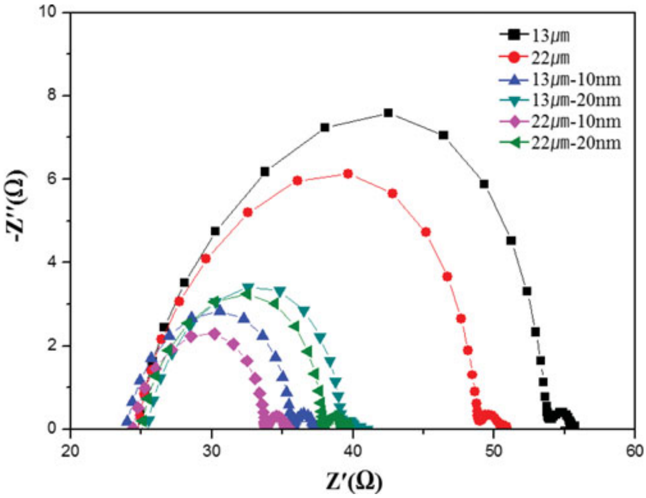

Figure 5. EIS Nyquist plots for DSSCs with various composite TiO_2 photoelectrodes.

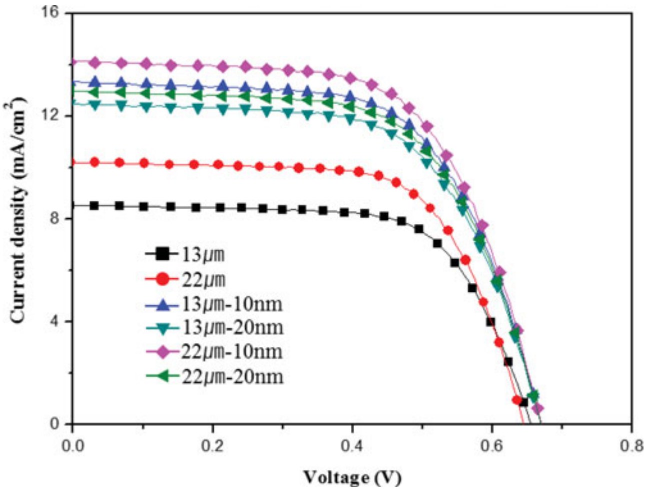

Figure 6. *I–V* characteristics of DSSCs.

charge recombination at the TiO_2/dye/electrolyte interface.[28,29] The reduction in R_{CT} means that there is a decrease in the recombination rate and indicates fast electron-transfer processes in the DSSC. Efficient charge-transfer paths decrease the recombination rate of electrons with I_3^- or the oxidizing dye, resulting in a high photocurrent density and conversion efficiency.[30]

Figure 6 shows the *I–V* photovoltaic performances of DSSCs with various structures under AM 1.5 illumination (100 mW/cm2). Table 1 summarizes the efficiencies, fill factors (FFs), open-circuit voltages (V_{OC}s), and integral photocurrents of the solar cells. For the photoelectrode with 10 nm TNPs spin-coated on 22 μm TNAs, the corresponding DSSC exhibited a high light-to-electric energy conversion efficiency of 5.91%, a short-circuit current density (*J*sc) of 14.10 mA/cm^2, a V_{OC} of 0.66 V, and a FF of 62.58%. These results indicate that J_{SC} increased significantly on addition of TNPs. It is speculated that deposition of TNPs on the TNAs in the DSSC increased the specific surface areas of the nanotubes, and the dye adsorption area was increased accordingly, resulting in a significant increase in the photoelectric conversion efficiency.

Table 1. Integral photocurrent densities (J_{SC}), open-circuit voltages (V_{OC}), fill factors (FF), and efficiencies (η) of DSSCs fabricated using various TiO_2 photoelectrodes

Sample	V_{OC} (V)	J_{sc} (mA/cm^2)	FF (%)	η
13 μm	0.65	8.52	67.38	3.76
22 μm	0.64	10.19	66.64	4.38
13 μm–10 nm	0.66	13.33	62.93	5.61
13 μm–20 nm	0.66	12.48	62.72	5.23
22 μm–10 nm	0.66	14.10	62.58	5.91
22 μm–20 nm	0.66	12.98	62.85	5.45

Conclusions

In this work, TNAs were fabricated using a three-step anodization process. DSSCs were constructed with TiO_2 films made from TNPs and TNAs, and the effects of various conditions on the resulting photoelectrodes were investigated. A light-to-electric energy conversion efficiency of 5.91% was achieved under simulated solar irradiation at 100 mW/cm^2 (AM 1.5). The DSSC based on a photoelectrode consisting of 10 nm TNPs coated on 22 μm TNAs gave a better photovoltaic performance (higher J_{SC}) than the cell fabricated with only TNAs. It was found that the conversion efficiency of the DSSC was greatly affected by increases in the specific surface area of the nanotubes, and the dye adsorption area increased accordingly. Additionally, using 10 nm TNPs was found to be effective for improving the efficiency of TiO_2-based DSSCs.

Acknowledgments

This work was supported by a Human Resources Development program (No. 20124030200010) of the Korea Institute of Energy Technology Evaluation and Planning (KETEP) grant, funded by the Korean Government Ministry of Trade, Industry, and Energy. This work was also supported by a National Research Foundation of Korea (NRF) Grant Funded by the Korean Government (MEST) (No. 2012R1A1A2044472).

References

[1] O'Regan, B., & Grätzel, M. (1991) *Nature 353*, 737.

[2] Lee, B., & Kim, J. (2009) *Curr. Appl. Phys. 9*, 404.

[3] O'Regan, B., & Grätzel, M. (1991) *Chem. Phys. Lett. 183*, 89.

[4] Durr, M., Schmid, A., Obermaier, M., Rosselli, S., Yasuda, A., & Nelles, G. (2005) *Nature 4* 607.

[5] Matsui, H., Okada, K., Kawashima, T., Ezure, T., Tanabe, N., Kwawano, R., & Watanabe, M. (2004) *J. Photochem. Photobiol. A-Chem. 164*, 129.

[6] Kim, S. S., Nah, Y. C., Noh, Y. Y., Jo, J., & Kim, D. Y. (2006) *Electrochim. Acta 51*, 3814.

[7] Robertson, N. (2006) *Angew. Chem. Int. Ed. 45*, 2338.

[8] Kang, S. H., Kim, J. Y., Kim, H. S., Koh, H. D., Lee, J. S. & Sung, Y. E. (2008) *J. Photochem. Photobiol. A-Chem. 200*, 294

[9] Jung, H. G., Kang, Y. S. & Sun, Y. K. (2010) *Electrochim. Acta 55*, 4637.

[10] Shin, S. G., Kim, K. H., Bark, C. W. & Choi, H. W. (2013) *Jpn. J. Appl. Phys. 52*, 11NM03.

[11] Chou, C. S., Guo, M. G., Liu, K. H. & Y. S. (2013) *Chen, Appl. Energy 92*, 224.

[12] Xu, C., Shin, P. H., Cao, L., Wu, J., & Gao, D. (2010) *Chem. Mater. 22*, 143.

[13] Stergiopoulos, T., Valota, A., Likodimos, V., Speliotis, Th., Niarchos, D., Skeldon, P., Thompson, G.E. & Falaras, P. (2009) *Nanotechnology 20*, 365601.

[14] Crossland, E. J. W., Nedelcu, M., Ducati, C., Ludwigs, S., Hillmyer, M. A., Steiner, U., & Snaith, H.J. (2009) *Nano Lett. 9*, 2813.

[15] Kang, T. S., Smith, A. P., Taylor, B. E. & Durstock, M. F., *Nano Lett. 9*, 601 (2009).

[16] Foong, T. R. B., Shen, Y., Hu, X., & Sellinger, A., *Adv. Funct. Mater. 20*, 1390 (2010).

[17] Yoon, J. H., Jang, S. R., Vittal, R., Lee, J., & Kim, K. J. (2006) *J. Photochem. Photobiol. A-Chem. 180*, 184.

[18] Kang, S. H., Choi, S. H., Kang, M. S., Kim, J. Y., Kim, H. S., Hyeon, T., & Sung, Y. E. (2008) *Adv. Mater. 20*, 54.

[19] He, W., Qiu, J., Choi, S. K., Kim, W. D., Lee, J. H., Kim, Y. D., Kim, S. H., Kim, H. K. & Hwang, Y. H. (2011) *Curr. Appl. Phys. 11*, S320.

[20] Park, J. H., Lee, T. W. & Kang, M. G., *Chem. Commun.* 2867 (2008).

[21] Yang, Z., Ma, Z., Pan, D., Chen, D., Xu, F., & Chen, S. (2014) *Ceram. Int. 40*, 173.

[22] Zhang, J., Li, S., Ding, H., Li, Q., Wang, B., Wang, X., & Wang, H., *J. Power Sources 247*, 807 (2014).

[23] Jin, Y. S., Kim, K. H., Park, S. J., Yoon, H. H. & Choi, H. W. (2010) *J. Korean Phys. Soc. 57*, 1049.

[24] Jin, Y. S., Kim, K. H., Park, S. J., Yoon, H. H., and Choi, H. W. (2011) *J. Nanosci. Nanotechnol. 11*, 10971.

[25] Keis, K., Magnusson, E., Lindstrom, H., Lindquist, S.E. & Hagfeldt, A. (2002) *Sol. Energy Mater. Sol. Cells 73*, 51.

[26] Stergiopoulos, T., Arbatzis, I.M., Cachet, H., & Falaras, P. (2003) *J. Photochem. Photobiol. A-Chem. 155*, 163.

[27] Yang, C. C., Zhang, H. Q. & Zheng, Y. R. (2011) *Curr. Appl. Phys. 11*, S147.

[28] Fabregat-Santiago, F., Bisquert, J., Palomares, E., Otero, L., Kuang, D., Zakeeruddin, S.M. & Grätzel, M. (2007) *J. Phys. Chem. C*, *111*, 6550.

[29] Kern, R., Sastrawan, R., Ferber, J., Stangl, R., & Luther, J. (2002) *Electrochim. Acta 47*, 4213.

[30] Zhong, M., Shi, J., Zhang, W., Han, H., & Li, C. (2011) *Mater. Sci. Eng. B-Adv. Funct. Solid-State Mater. 176*, 1115.